Chemical Synthesis, Characterization, and Properties of Conducting Copolymers of Imidazole and Pyridine

V. Raj,[1] D. Madheswari,[2] M. Mubarak Ali[1]

[1]*Department of Chemistry, Periyar University, Salem, 636011 Tamil Nadu, India*
[2]*Department of Chemistry, Government Arts College for Women, Salem, 6363008 Tamil Nadu, India*

Received 12 April 2011; accepted 5 July 2011
DOI 10.1002/app.35190
Published online 20 October 2011 in Wiley Online Library (wileyonlinelibrary.com).

ABSTRACT: A series of conducting copolymers were synthesized by chemical oxidative polymerization of imidazole (Imi) and pyridine (Py) in acetonitrile medium at ambient temperature. The yield, solubility, and conductivity of the copolymers were measured by changing the Imi/Py molar ratio from 0/100 to 100/0. The as-prepared Imi/Py conducting copolymers were characterized by UV-Visible, FTIR, ^{1}H-NMR, DSC, TGA, and XRD. The results suggest that the resulting copolymers were more easily soluble in most of the organic solvents than in polyimidazole. The polymer obtained is a real copolymer containing imidazole and pyridine units, but the Imi content calculated on the basis of the proton NMR spectra is lower than feed Imi content. The thermostability of the Imi/Py copolymer increases with increasing Imi unit content. The copolymers show comparatively higher conductivity and higher thermal stability than the homopolymer polypyridine and are lower than those of polyimidazole. © 2011 Wiley Periodicals, Inc. J Appl Polym Sci 124: 1649–1658, 2012

Key words: conducting polymers; copolymers; differential scanning calorimeter; X-ray; FTIR

INTRODUCTION

Aromatic nitrogenous polymers have attracted much attention recently because they exhibit multiple functionality such as excellent electroconductivity and high gas separation ability.[1] The synthesis and investigation of π-conjugated copolymers with structures A and B have attracted considerable interest in recent years.[2] The wide range of aromatic building blocks that can be used offer considerable opportunities for development of novel conductive materials.

Type A polymers (Fig. 1) are normally obtained by electrochemical or chemical oxidation of the corresponding monomer unit compound with linkages occurring predominantly through the 2 and 5 positions.[3–13] Type B polymers, on the other hand, are usually obtained by a chemical coupling route.[14–19]

Pyridine-based conducting polymers have been attracting increasing interest in recent years because of their facile *n*-doping[20–23] and their ability to bind metal ions. Poly(pyridine-2,5 diyl) s are prepared by Ni (0) catalyzed dehalogenation of polycondensation of dibromo-pyridine and 2,2′-bipyridines.[23] There have been several reports on copolymerization of pyridine with thiophene, *N*-methyl pyrrole, and selenophene.[8,24–26] As far as we know, copolymerization of pyridine and imidazole have not previously been reported. We report here on copolymers prepared by oxidative polymerization of imidazole and pyridine. The π-conjugated polymers have been attracting increasing attention recently because of envisaged application in microelectronics and super capacitors.[27,28] Pyridine-containing polymers have been of particular interest as they are used as *n*-doped organic semiconductors.[28]

Correspondence to: V. Raj (alaguraj2@rediffmail.com).

Journal of Applied Polymer Science, Vol. 124, 1649–1658 (2012)

EXPERIMENTAL

Materials

Imidazole (Imi), analytical reagent grade (Himedia), pyridine (Py; Lobachemie), and ammonium persulfate (Rankem) were commercially obtained and used as received. Acetonitrile (Merck) was freshly distilled prior to utilization. All other solvents $CHCl_3$ (E-Merck), DMF (E-Merck), DMSO (E-Merck), Methanol (Qualigens) were of analytical grade and used as received.

Copolymerization

Imi/Py copolymers were prepared by oxidative polymerization by using a previously described method which was used for the synthesis of pyrrole and anisidine copolymers, pyrrole and *m*-toluidine copolymers.[29–32] The exact procedure used for the preparation of the Imi/Py (40/60) copolymer is as follows: To 100 mL of the 95% acetonitrile solution,

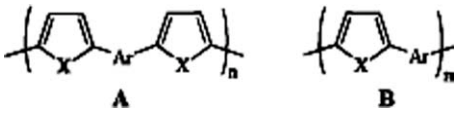

Figure 1 Type A and Type B polymers.

0.2723 g (4 mmol) imidazole and 0.4746 g (6 mmol) pyridine were added to a 250-mL glass flask and stirred vigorously for one hour. Ammonium per sulfate [$(NH_4)_2S_2O_8$], 2.964 g (13 mmol), was dissolved separately in 30 mL of 95% acetonitrile to prepare an oxidant solution. The monomer solution was added with the oxidant solution dropwise at a rate of one drop for every 3 s at room temperature (30°C) (the total molar ratio is monomer/oxidant = 1/1). Immediately, after the first few drops, the reaction solution turned milky white. The reaction mixture was stirred for 24 h at ambient temperature. The reaction mixture was then added to 200 mL of methanol (as a nonsolvent) to precipitate out the copolymer. The milky white precipitate obtained was filtered and washed with excess of water to remove the oxidant and oligomers. The milky white powder was dried under vacuum for 72 h. The copolymer of 1.577 g was obtained with a yield of 68%.

Measurements

The solubility of the synthesized copolymers was tested using the following method: Polymer powder sample of 5 mg was added into the solvent of 0.5 mL and dispersed thoroughly. After the mixture was swayed continuously for 24 h at room temperature (30°C), the solubility of the polymers was characterized. UV-visible absorption spectra were recorded using a Perkin–Elmer UV-Visible Spectrometer using 0.5 cm path quartz cells in the range 200–1100 nm. FT-IR spectrum of the polymer was recorded on Perkin–Elmer FT-IR spectrometer with KBr pressed pellet.

^{1}H-NMR spectra were recorded in $CDCl_3$ solution with a Brucker AC 200 spectrometer, at 200 MHz. All the chemical shifts (∂ in ppm) were referenced to tetramethyl silane (TMS). Dry Imi/Py powder was compressed into pellets, 13 mm in diameter and 1 mm thick, and the conductance was measured by four-probe method (using four probe resistvity setup) at various temperatures ranging from 308 to 368 K.

Thermal studies (TGA and DSC) were carried out in the temperature range of 50–800°C with Mettler TA 3000 Analyzer and TGA-DSC 910S differential scanning calorimeter. The measurement was performed at a heating rate of 10°C/min with the sample size of 5–10 mg in nitrogen atmosphere. XRD was performed on a Phillips X-ray diffractometer using Cu kα radiation source operating at 50 kV and 30 mA.

RESULTS AND DISCUSSION

Synthesis of copolymers

The imidazole-pyridine copolymer was synthesized by oxidative polymerization using respective monomers and ammonium persulfate as oxidant in acetonitrile. The progress of the copolymerization reaction was monitored by testing the solution temperature. It was found that on dropping oxidant solution slowly and regularly, the polymerization solution temperature increases and finally reaches a nearly constant temperature.

It was found that the copolymerization yield of imidazole and pyridine was dependent on the monomer ratio as shown in Table I. The yield decreased with increase in feed Imi content. The Imi/Py copolymerization shows the minimal yield at feed Py content of 20 mol %, but the highest yield at the feed Py content was 80 mol %. An introduction of less than 20 mol % pyridine monomer might retard the polymerization of imidazole and result in difficulty in the formation of higher molecular weight copolymer.

As shown in Table II by increasing the polymerization temperature from −5 to 26°C the

TABLE I
Effect of Imi/Py Molar Ratio on Solubility of Imi/Py Copolymers

			Solubility in solvents[a]					
Imi/Py molar ratio	Conductivity S cm^{-1}	Yield (%)	NMP	DMF	DMSO	THF	$CHCl_3$	C_6H_6
0/100	4.76×10^{-5}		MS	MS	MS	MS	MS	IS
20/80	2.15×10^{-4}	69	MS	MS	MS	PS	PS	S
40/60	8.38×10^{-4}	68	MS	MS	MS	PS	PS	PS
50/50	1.327×10^{-3}	66	MS	MS	MS	PS	PS	IS
60/40	1.676×10^{-3}	65	MS	MS	MS	S	PS	IS
80/20	1.89×10^{-3}	64	MS	MS	MS	S	SS	IS
100/0	1.9×10^{-3}		MS	MS	MS	SS	SS	IS

[a] IS: Insoluble; MS: major soluble; PS: partially soluble; S: soluble; SS: slightly soluble.

TABLE II
The Effect of Polymerization Temperature and the Effect of Monomer Oxidant Ratio on the Polymerization Yield of Copolymer Imi/Py (50/50) in Acetonirile

Polymerization temperature (°C)	Yield (%)	Monomer/oxidant/ Feed molar ratio	Yield (%)
−5	18	10/2	19
0	19		
5	19	10/5	42
15	20		
26	30	10/10	95

polymerization yield increased. It appears that 26°C is most suitable for the preparation of higher molecular weight Imi/Py (50/50) copolymer due to higher chain terminating rate of oxidative polymerization from imidazole monomer.

The effect of monomer/oxidant (ammonium per sulfate) molar ratio on the copolymerization of Imi/Py (50/50) in acetonitrile solution at ambient temperature was studied. It can be seen from Table II that with increasing molar ratio of monomer over oxidant, the copolymerization yield decreases significantly. When less oxidant was added, the oxidant will be consumed fast and some monomer cannot be further oxidized to polymerize, leading to low polymerization yield.

Solubility of the copolymers

It can be seen from Table I that with increasing pyridine content, the Imi/Py copolymers exhibit an enhanced solubility in the six solvents. Finally, it was found that Imi/Py (20/80), (40/60), and (50/50) copolymers were completely soluble in NMP, DMF, and DMSO and partially soluble in $CHCl_3$ and THF. It should be noted that the Imi/Py (80/20) copolymer with the lowest feed pyridine content exhibits more solubility than Imi/Py (60/40) copolymer. Thus, it could be considered that the improvement in the copolymer solubility with increasing pyridine content is due to the change in molecular structure. These observations confirm that the oxidative copolymerization between Imi and Py monomers has occurred. As compared with Imi homopolymer, an improvement in solubility of 20/80 copolymer in

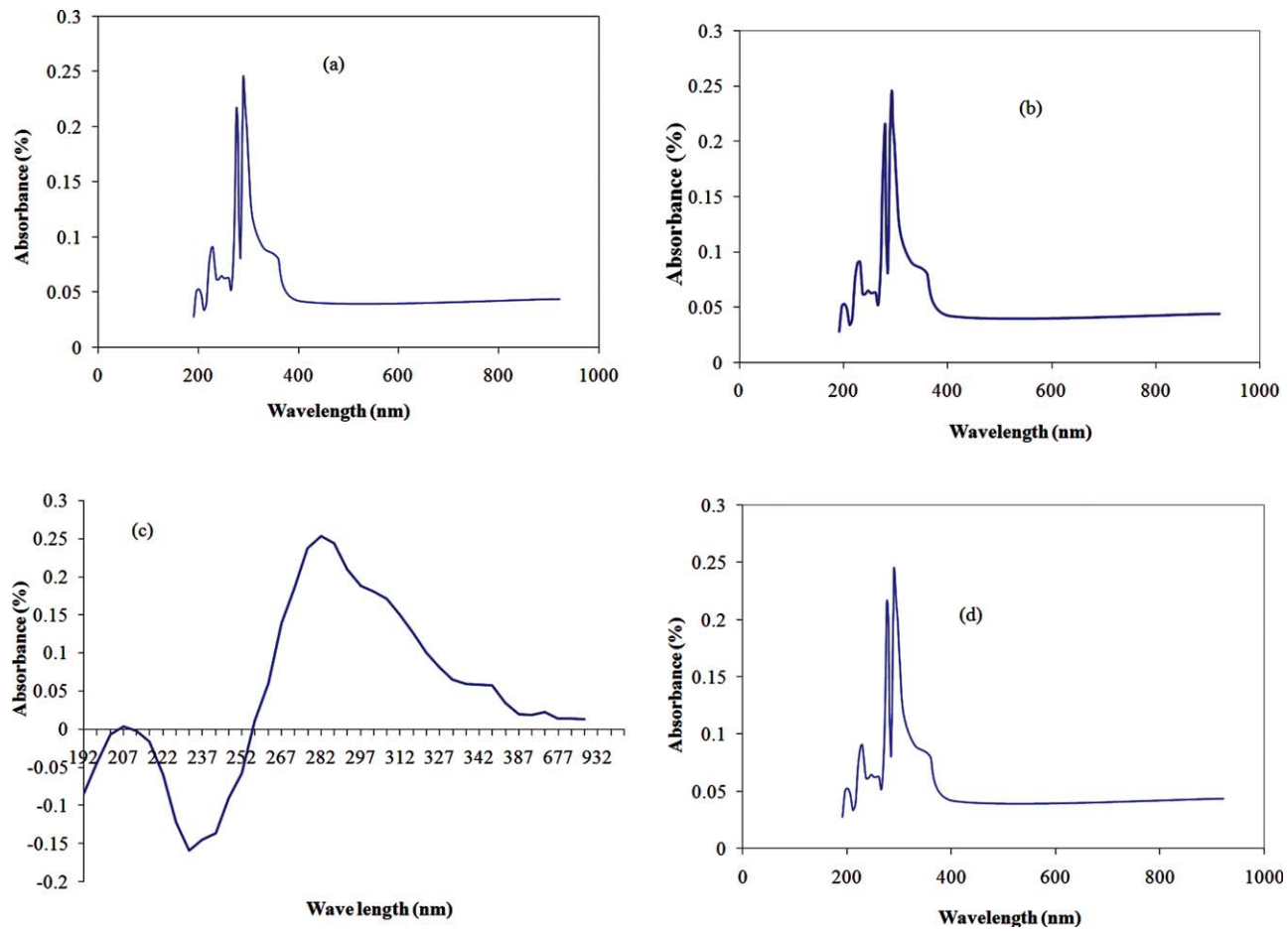

Figure 2 UV-visible spectra of Imi/Py copolymer with of monomer ratios: (a) 20/80; (b) 50/50; (c) PImi; (d) PPy [Color figure can be viewed in the online issue, which is available at wileyonlinelibrary.com.]

TABLE III
Variation of UV-Vis Spectra of Copolymers with Various Imi/Py Molar Ratios

	Wavelength (nm)		
Feed Imi/Py molar ratio	Strong band		Weak band
0/100	282	–	235
20/80	293	280	232
40/60	292	278	231
50/50	291	277	230
100/0	302	–	–

chloroform and tetrahydrofuran is due to the relatively irregular molecular structure that results from an incorporation of pyridine moieties into the imidazole polymer chain.

UV-Visible spectra of the copolymers

Figure 2(a–d) show the UV-Vis absorption spectra of two copolymer solutions with Imi/Py ratios 20/80, 50/50, Pimi and Ppy in chloroform. The absorption bands of all the copolymers are listed in Table III. A strong band and a weak band are observed. It can be seen from Table III that the wavelength of both the bands moves to lower value with increasing feed Imi content.[33] Additionally, the relative intensity of the weak band becomes weak further with increasing Imi content. The continuous variation of wavelength and intensity of UV-Vis bands may result from the copolymerization effect of imidazole with pyridine. In other words, the polymer formed by oxidative polymerization of imidazole with pyridine is the copolymer of two monomers rather than the mixture of two homopolymers. A similar variation of UV-Vis spectral characteristics was observed for the pyrrole/*o*-anisidine copolymer solution in DMSO.[34]

The strong absorption band that appears in the wavelength range of 291–302 nm is due to the imidazole moiety of the copolymer and a strong band and weak band appearing at 282–277 nm and 235–230 nm are due to the pyridine moiety of the copolymer.

FT-IR spectra of the copolymers

Representative FT-IR spectra of the copolymers with Imi/Py molar ratios of 50/50 (a), 20/80 (b), PImi (c), and Ppy (d) are shown in Figure 3. Poly(imidazole) exhibits —NH— vibration weak peak at 3077 cm^{-1} and C=N— stretching peak at 1451 cm^{-1}. Poly (pyridine) exhibits —NH— vibration weak peak at 3138 cm^{-1} and C=N— stretching band at 1660–1430 cm^{-1}. A broad and weak band centered at 3052 cm^{-1} due to characteristic *N*—H stretching vibration suggests the presence of —NH— groups

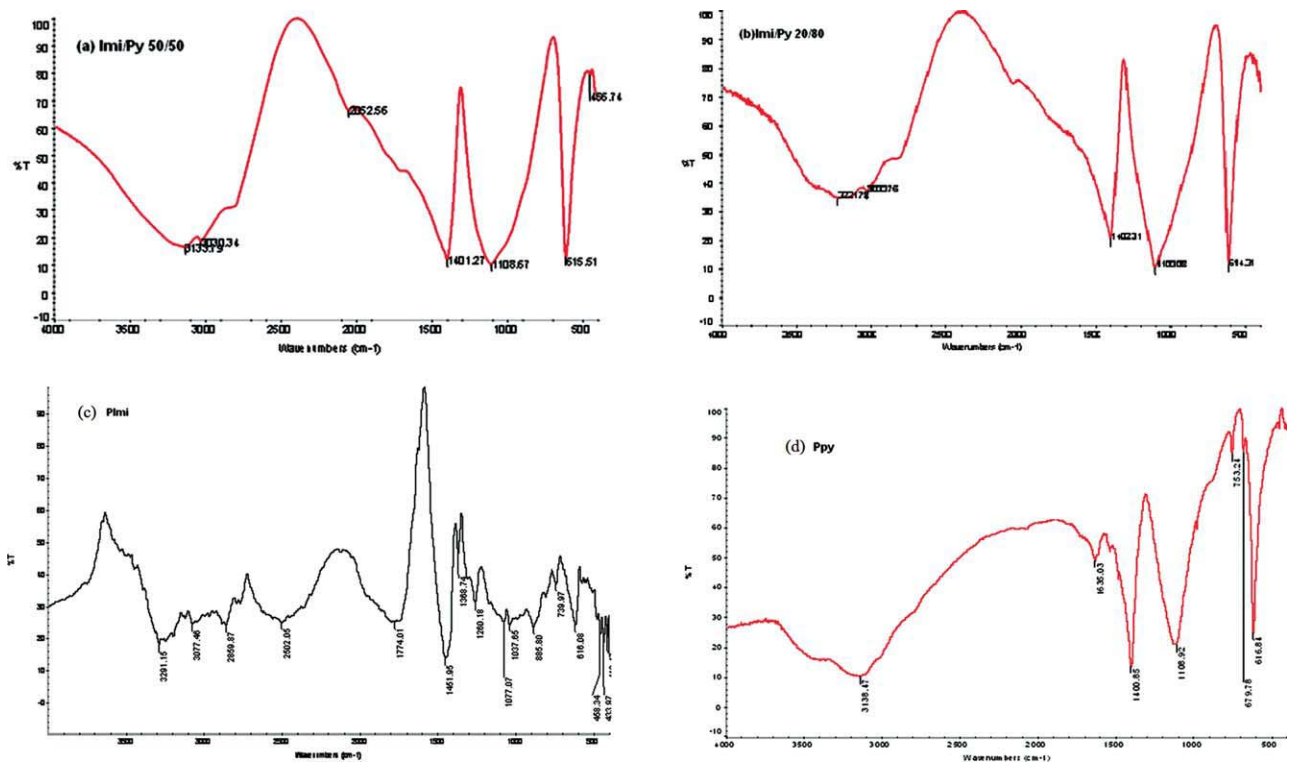

Figure 3 Fourier transform infrared (FTIR) spectra of Imi/Py copolymers with monomer ratios: (a) 50/50; (b) 20/80; (c) PImi; (d) Ppy [Color figure can be viewed in the online issue, which is available at wileyonlinelibrary.com].

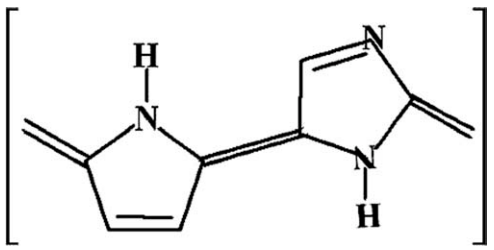

Figure 4 Quinoid form of imidazole unit.

and a sharp band at 1432 cm^{-1} is due to C=N— stretching in Imi and Py units. This weak band becomes broader and lower resolution with an increase in Py feed content from 0 to 100 mol %. Two weak peaks at 3080 and 3010 cm^{-1} are due to aromatic C—H stretching vibrations. On increasing the feed Imi content to higher than 50%, these two peaks become weaker because Imi unit contains less aromatic C—H bond and does not contain aliphatic C—H bond. Thus, the characteristics of IR absorption spectra of Imi/Py copolymers above 2000 cm^{-1} are dominated by the Py unit. However, the absorption below 2000 cm^{-1} is obviously influenced by the Imidazole units. On comparison of the spectra of poly(imidazole), poly(pyridine), and Imi/Py copolymers, the copolymer spectra exhibit some differences in the relative absorbance and wave number. With increasing feed Imi content, the relative absorption intensity at 1625–1604 cm^{-1} and 1492–1450 cm^{-1} gets stronger significantly. This should be attributable to Imi unit to some extent because the bands[35–37] at 1625–1592 cm^{-1} and 1454–1441 cm^{-1} are characteristic of poly(imidazole). On the contrary, the characteristic absorption of Py unit at 1600, 1430, 748, and 703 cm^{-1} becomes very weak significantly with increasing feed Imi content from 0 to 100 mol %. The absorption at 1592 cm^{-1} increases significantly with increasing feed Imi content suggesting that the Imi unit in the polymer chains seems to exist mainly in the following quinoid form.[38] (Fig. 4) The difference of wave number might result from the copolymerization effect of imidazole and pyridine.

^{1}H-NMR spectra of the copolymers

Figure 5(a–d) show the ^{1}H-NMR spectra of the copolymers of imidazole and pyridine 50/50: (a) 80/20, (b) PImi, (c) Ppy, and (d) in DMSO. The spectra of the copolymers exhibit peaks, arising due to both poly(imidazole) and poly(pyridine) units. The six membered hetero aromatic proton of pyridine (C_4) appears at 7.5 ppm. The signal at 7.09 ppm is due to the proton of the pyridine ring and the proton of terminal pyridine ring is observed at 8.5 ppm ($C_{2,6}$). The signal at 7.2 ppm (C_4) is due to the proton of imidazole ring and peak at 7.8 ppm (C_2) is due to the proton of the terminal imidazole ring.

^{1}H-NMR analysis of Imi/Py copolymer disclosed that oxidative coupling essentially occurred as anticipated in second and sixth position of pyridine moieties and second and fifth position of imidazole

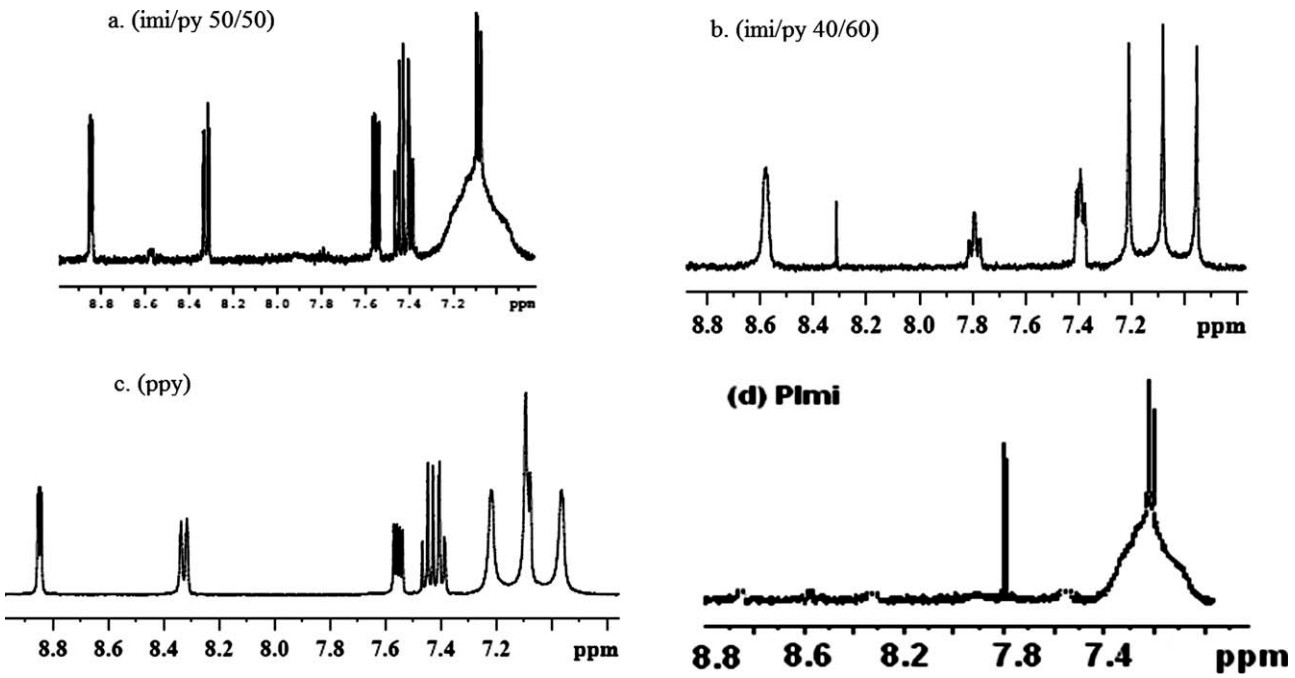

Figure 5 ^{1}HNMR spectra of the copolymers with Imi/Py molar ratio of (a) 50/50, (b) 80/20, (c) Ppy, (d) Pimi in DMSO at 400 MHz.

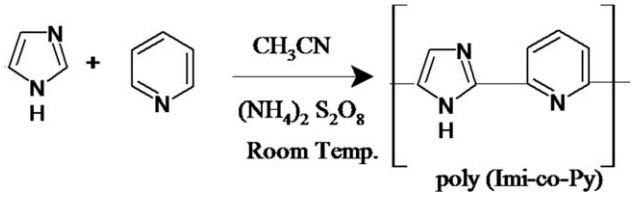

Figure 6 Schematic diagram of formation of copolymer Imi/Py from its monomers.

moiety. It is consistent with the expected structure. As polymerization proceeds, the second and sixth proton peaks of pyridine at 8.5 ppm disappear. No abnormal linkages resulting from 3,5 coupling (reaction is given in Fig. 6) were detected in the ^{1}H-NMR spectra of copolymers.

It can be seen that the aromatic protons of pyridine are sifted slightly downfield in the spectra of the copolymers, whereas protons of poly(imidazole) does not show much shift. The downfield shift of aromatic protons of pyridine could be attributed to a decrease in the electron density of the ring. ^{1}H-NMR spectra of Imi/Py copolymers do not change systematically with increasing feed Imi content.

The ratio of proton area of Imi over Py is 1/3

Based on the comparison of area of proton peaks of the pyridine and imidazole, the ratio of Imi/Py units in the copolymers have been calculated and listed in Table III. It seems that the actual Imi content is slightly lower than the feed imi content for Imi/Py copolymers. The difference in Imi content should be due to the lower solubility of polyimidazole in $CHCl_3$ as listed in Table I. A similar trend has been observed in the Imi/Cz copolymers.[39]

TABLE IV
Composition of Imidazole and Pyridine in the Copolymer

	Feed composition in mole fraction			Copolymer composition in mole fraction	
Sample no.	Imidazole, M_1	Pyridine, M_2	$c^* = I_{Imi}/I_{Py}$	Imidazole, m_1	Pyridine, m_2
1	0.00	1.00	–	–	–
2	0.20	0.80	0.09	0.19	0.81
3	0.40	0.60	0.19	0.36	0.64
4	0.50	0.50	0.24	0.42	0.58
5	0.60	0.40	0.49	0.56	0.44
6	0.80	0.20	1.10	0.77	0.23
7	1.00	0.00	–	–	–

* Obtained from ^{1}NMR spectra of the copolymer samples.

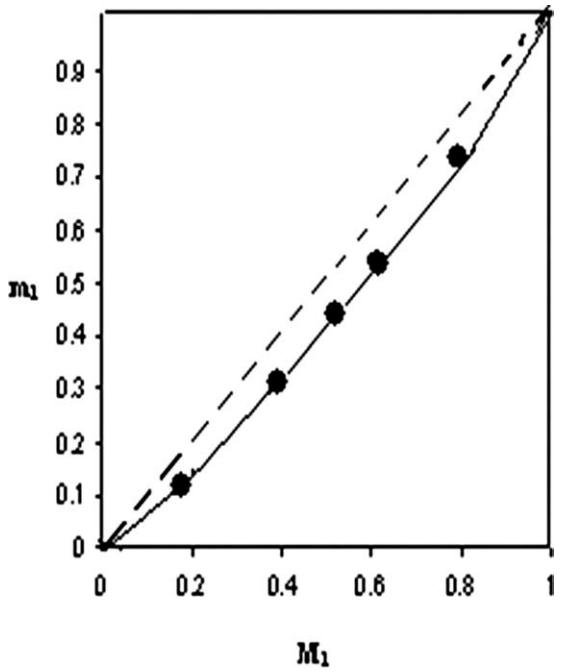

Figure 7 Plot of mole fraction of Imidazole in the feed versus that in copolymer.

Copolymer composition

The composition of Imi/Py copolymers were determined from the ^{1}H-NMR spectra using the following relation:

$$m_1 = 3c/1 + 3c$$

where m_1 is the mole fraction of Imi in the copolymer.

c = intensities of Imi protons/intensities of Py protons.

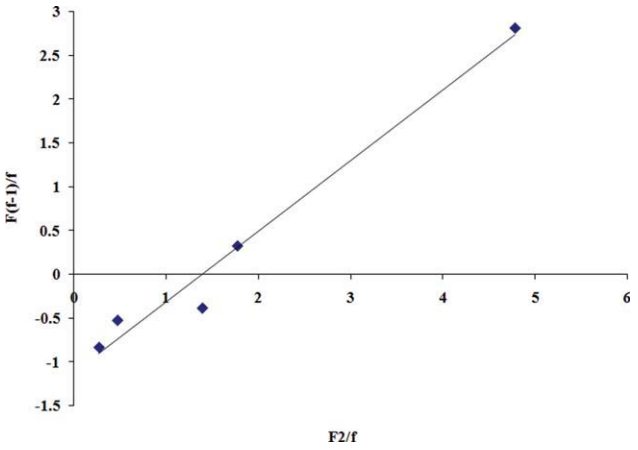

Figure 8 Fineman-Ross plot for imidazole-pyridine copolymer system.

TABLE V
Fineman-Ross and Kelen-Tudos Parameters for the Copolymerization of Imidazole and Pyridine

			Fineman-Ross parameters		Kelen-Tudos parameters	
Sample no.	M_1 ($F = M_2$)__	m_1 ($f = m_2$)	$G = F(f-1)/f$	$H = F^2/f$	$\eta = G/(\alpha + H)$	$\xi = H/(\alpha + H)$
1	0.25	0.23	−0.84	0.27	−0.54	0.17
2	0.67	0.56	−0.53	0.47	−0.30	0.27
3	1.00	0.72	−0.39	1.39	−0.15	0.52
4	1.50	1.27	0.32	1.77	0.104	0.58
5	4.00	3.35	2.81	4.78	0.463	0.79

M_1 = Imidazole; M_2 = Pyridine; $\alpha = \sqrt{H_{min}}$; $H_{max} = 1.29$.

The data on the monomer feed composition determined by using the above relation are presented in Table IV. To ascertain the normal copolymer kinetic behavior, a plot was drawn (Fig. 7) between the mole fraction of Imi in the feed versus that in the copolymer. The nature of the plot suggests that there is a strong tendency for random distribution of monomers in the copolymer chain.

Determination of reactivity ratios

Reactivity ratio also plays a vital role in deciding the composition of monomer in the copolymers. The reactivity ratios of Imi (M_1) and Py (M_2) were determined from the monomer feed ratios and the resultant copolymer compositions determined by ^{1}H-NMR analysis, using Fineman-Ross and Kelen-Tudos equations (Table V).

According to Fineman-Ross, the reactivity ratios of monomers 1 and 2 in the copolymer can be determined by the plot of F^2/f versus $F(f-1)/f$. The plot should be a straight line with the slope equal to r_1 and the intercept at $F^2/f = 0$ equal to r_2. (Fig. 8).

A similar graphical linear equation is proposed by Kelen-Tudos to determine the reactivity ratio. The plot of η versus ξ (Fig. 9) is a straight line with the intercept at $\xi = 0$ equal to $-r_2/\alpha$ and intercept at $\xi = 1$ equal to r_1.

Here r_1 and r_2 are the reactivity ratios of monomer 1 (Imi) and monomer 2 (Py), respectively. The reactivity ratios obtained from the FR (Fig. 8) and KT (Fig. 9) plots are

$r_1 = 0.81$; $r_2 = 1.17$ (FR method)

$r_1 = 0.79$; $r_2 = 1.16$ (KT method)

The product of r_1 and r_2 (0.94 and 0.92) suggest the random distribution of monomeric units in the copolymer chain.

Thermal analysis

Representative TGA and DTG curves of Imi/Py copolymers with three Imi/Py ratios of 40/60 (a), 50/50 (b), and 60/40 (c) are shown in Figure 10, from which a series of thermal degradation parameters are obtained and listed in Table VI. The copolymers lost their weights gradually with increasing temperature from 200 to 300°C and more rapidly from 300 to 500°C. On increasing Imi content from 0 to 100 mol %, the temperature at which the second maximum weight loss and char yield increases to 700°C, suggesting that the char yield at elevated temperature could be attributed to Imi unit in the copolymer. These results indicated that the thermal stability of the Imi/Py copolymer increases with increasing Imi unit content.

The DSC scans of the Imi/Py copolymers with ratios of 40/60 (a) and 60/40 (b) are shown in Figure 11. All these curves show a sharp decomposition peaks at 228, 336, and 363°C for Imi/Py (40/60) and at 346, 364, and 375°C for (60/40) copolymers, respectively. The peaks appearing at 228–346°C and 364–375°C are assigned to the interchain crosslinking in the polymer.

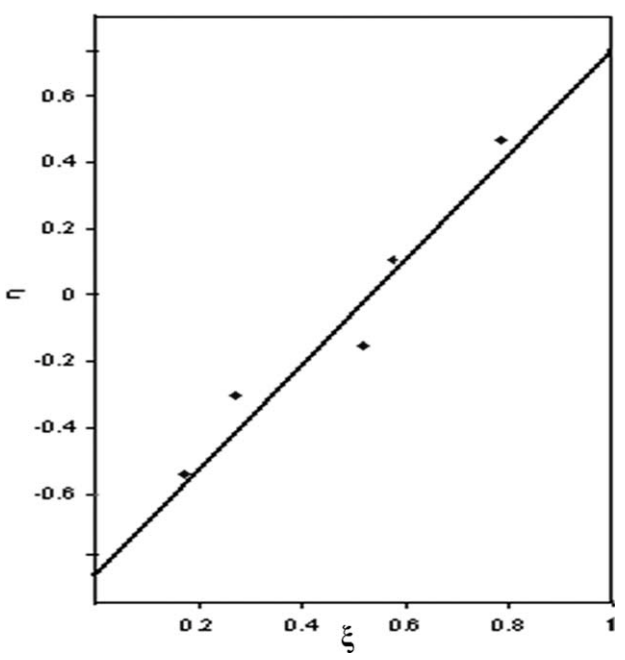

Figure 9 Kelen-Tudos plot for imidazole-pyridine copolymer system.

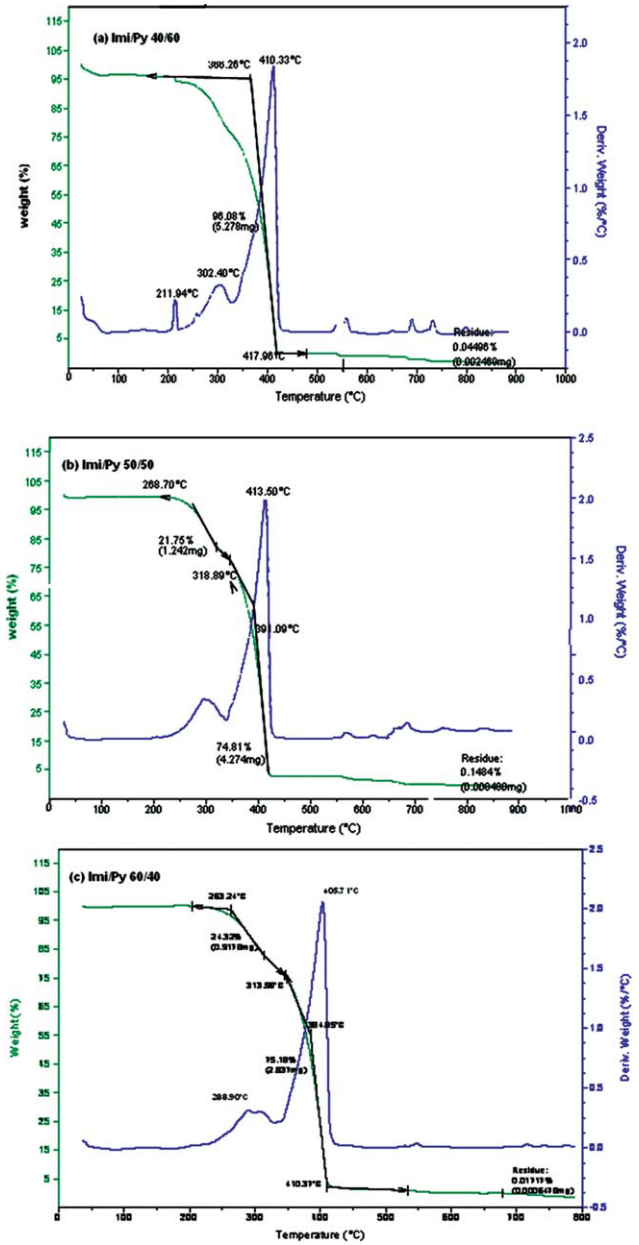

Figure 10 TGA/DTG curves of copolymers with Imi/Py monomer ratios 40/60, 50/50, 60/40 [Color figure can be viewed in the online issue, which is available at wiley onlinelibrary.com].

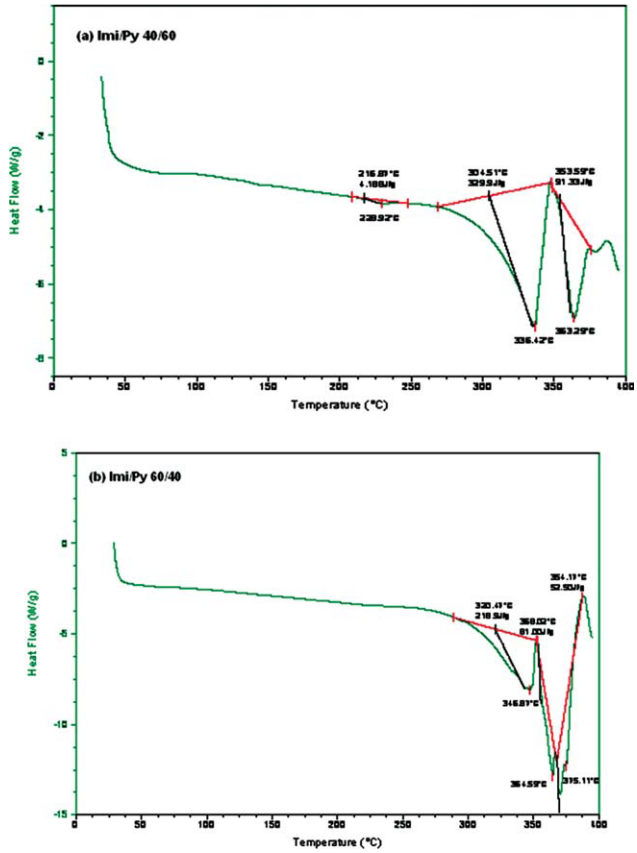

Figure 11 Differential scanning calorimetric analysis of copolymers with Imi/Py molar ratios of (a) 40/60 and (b) 60/40 [Color figure can be viewed in the online issue, which is available at wileyonlinelibrary.com].

In TGA of polyimidazole, the transition of pure PImi at 373°C with 53% weight loss is due to morphological changes in the polymer. In DSC of pure polyimidazole an exothermic peak at 143°C is due to the removal of water dopant molecules present in the polymer and the other exothermic peak at 412°C is assigned to interchain crosslinking in the polymer. Thermal analysis data also suggest that the homopolymer polyimidazole is more stable compared to the copolymer Imi/Py and homopolymer polypyridine.

TABLE VI
Thermal Parameters of Copolymers

Copolymer Imi/Py	Weight loss (%)			Maximum decomposition temperature (°C)	Range of decomposition temperature (°C)
	200–300°C	400–500°C	Residue temperature (°C)		
0/100				193, 300	100–400
40/60		91.0	0.045	366, 534	400–540
50/50	21.7	74.8	0.1484	268, 380,660	200–660
60/40	24.3	75.2	0.0446	263, 384,678	200–680
100/0	–	86.0	3.34	373	300–420

X-ray diffraction

The XRD pattern of the copolymer Imi/Py (50/50), PPy, and PImi is shown in Figure 12. In the XRD pattern of the copolymer, there are four main peaks at 2θ = 20.7°, 29.0°, 29.4°, and 33.9° and five small peaks at 39°, 42°, 47°, 52°, and 62°. The peak centered at 2θ = 20.7° may be ascribed to the periodicity parallel to the polymer chain, while the weak peaks at high angles may be caused by the periodicity perpendicular to the polymer chain. The diffraction pattern of PImi has a peak at about 2θ = 20.2° which is a characteristic peak of poly(imidazole) which is shifted slightly to high angle in the copolymer. Appearance of sharp peaks shows the crystalline nature of the copolymer. This is also evidenced by our previous report. The crystallite size of both the homopolymer and copolymer were also calculated using Debye Scherer's formula (for copolymer = 49 nm, polyimidazole = 1.80 nm, polypyridine = 8.5 nm).

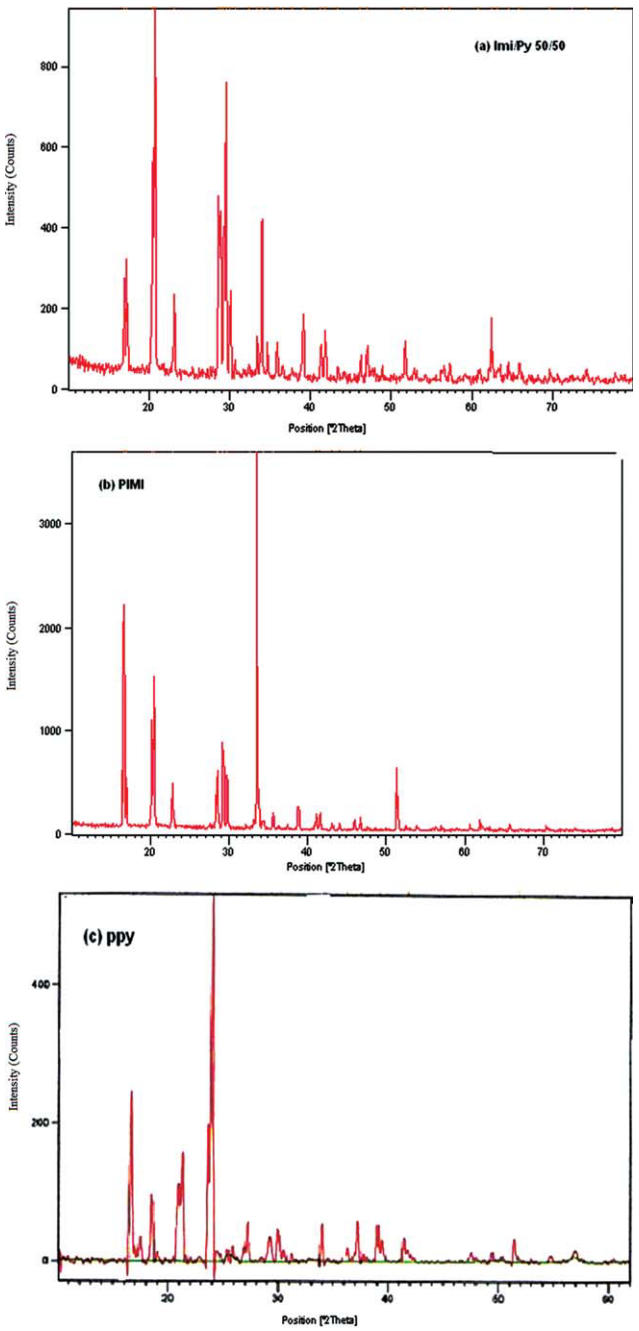

Figure 12 Powder X-ray diffraction pattern of copolymer Imi/Py (50/50), PImi and Ppy [Color figure can be viewed in the online issue, which is available at wileyonline library.com].

TABLE VII
Electrical Conductivity of Copolymer (50/50) at Different Temperatures

Temperature (°C)	Conductivity (S cm^{-1}) × 10^{-3}
35	2.54
45	2.76
55	3.53
65	3.74
75	5.34
85	7.25
95	9.09

Electrical conductivity

The electrical conductivity of the copolymer was measured on pellets at room temperature (30°C) by using the four probe method of Vander Pauw[61] pressed at 2 T cm^{-2}. The conductivity of the copolymers is given in Table VII. The conductivity of various copolymers lies in the narrow region of 2.5 × 10^{-4} to 5.48 × 10^{-5} S cm^{-1}. The conductivity of all the copolymers is found to be higher than that of polypyridine (2.68 × 10^{-5}) and polyimidazole (1.9 × 10^{-3}) S cm^{-1}. The conductivity of the copolymers increases with increase of imidazole content. The higher conductivity of the copolymers compared to that of the PPy homopolymer indicates the lowering of the band gap in the copolymers. This increase in conductivity with lowering of pyridine content in the comonomer feed suggests that the donor-acceptor type of interactions are dependent on the composition of the copolymer.[38] It is evident from Table VII that conductivity increases steadily with increase in temperature showing semiconductor behavior.

CONCLUSIONS

A series of the copolymers from imidazole and pyridine have been synthesized successfully by oxidative polymerization in acetonitrile medium at ambient temperature. UV-Visible, FT-IR, and ^{1}HNMR measurements suggest that the polymers obtained are actual copolymers consisting of two monomer units. XRD and DSC measurements indicate that the copolymers are crystalline. The copolymers exhibit

higher conductivity, higher thermal stability, and good solubility in various solvents than the homopolymer poly(pyridine).

References

1. Li, X. G.; Huang, M. R. J Appl Polym Sci 1997, 66, 2139.
2. Krivoshei, I. V.; Skorobogatov, V. M. Polyacetylene and Polyarylenes Synthesis and Conductive Properties; Gordon and Breach: Philadelphia, PA; 19 Polymer Monographs, Vol. 10, 1991.
3. Reynolds, J. R.; Katritzky, A. R.; Soloducho, J.; Belyakov, S.; Sotzing, G. A.; Pyo, M. Macromolecules 1994, 27, 7225.
4. Tanaka, S.; Sato, M.-A.; Kaeriyama, K. J. Macromol Sci Chem 1987, A24, 749.
5. Pelter, A.; Maud, J. M.; Jenkins, I. H.; Sadeka, C.; Coles, G. Tetrahedron Lett 1989, 30, 3461.
6. Ruiz, J. P.; Dharia, J. R.; Reynolds, J. R.; Buckley, L. J Macromol 1992, 25, 849.
7. Tanaka, S.; Kaeriyama, K. Polym Commun 1990, 31, 172.
8. Tanaka, S.; Kaeriyama, K. Makromol Chem Rapid Commun 1988, 9, 743.
9. McLeod, G. G.; Mahboubian-Jones, M. G. B.; Pethrick, R. A.; Watson, S. D.; Truong, N.; Galin, J. C.; Francois, J. Polymer 1986, 27, 455.
10. Ferraris, J. P.; Andrus, R. G.; Hrncir, D. C. J. Chem Soc Chem Commun 1989, 1318.
11. Ferraris, J. P.; Hanlon, T. P. Polymer 1989, 30, 1319.
12. Lorcy, D.; Cava, M. P. Adv Mater 1992, 4, 562.
13. Musmanni, S.; Ferraris, J. P. J. Chem Soc Chem Commun 1993, 172.
14. Bracke, W. J Polym Sci Part A Polym Chem 1972, 10, 975.
15. Montheard, J. P.; Pascal, T.; Seytre, G.; Steffan-Boiteaux, G.; Douillard, A. Synth Met 1984, 9, 389.
16. Pelter, A.; Rowlands, M.; Jenkins, I. H. Tetrahedron Lett 1987, 28, 5213.
17. Pouwer, K. L.; Vries, T. R.; Havinga, E. E.; Meijer, E. W.; Wynberg, H. J.;Chem Soc Chem Commun 1988, 1432.
18. Yamamoto, T.; Shimura, M.; Osakada, K.; Kubota, K. Chem Lett 1992, 1003.
19. Maruyama, T.; Kubota, K.; Yamamoto, T. Chem Lett 1992, 1827.
20. Yamamoto, T.; Ito, T.; Sanechika, K. Synth Met 1988, 25, 103.
21. Onoda, M. J Appl Phys 1995, 78, 1327.
22. Miyamae, T.; Yoshimura, D.; Ishii, H.; Ouchi, Y.; Saki, K.; Miyazaki, T.; Koike, T.; Yamamoto, T. J Chem Phys 1995, 103, 2738.
23. Yamamoto, T.; Maruyama, T.; Zhou, Z.-H.; Ito, T.; Fukuda, T.; Yoneda, Y.; Begum, F.; Ikeda, T.; Sasaki, S.; Takezoe, H.; Fukuda, A.; Kubota, K. J Am Chem Soc 1994, 116, 4832.
24. Tanaka, S.; Sato, M. A.; Kaeriyama, K. J. Macromol Sci Chem 1987, A24, 749.
25. Higgins, S.; Crayston, J. A. Synth Met 1993, 55, 879.
26. Jenkins, I. H.; Salzner, U.; Pickup, P. G. Chem Mater 1996, 8, 2444.
27. Guerrero, D. J.; Ren, X. M.; Ferraris, J. P. Chem Mater 1994, 6, 1437.
28. Shi, G. Q.; Yu, B.; Xue, G.; Shi, J. B.; Li, C. J Chem Soc Chem Commun 1994, 2549.
29. Li, X. G.; Huang, M. R.; Li, F.; Cai, W. J.; Jim, A.; Yang, Y. L. J Polym Sci 2000, 75, 458.
30. Li, X.-G.; Huang, M.-R.; Yang, Y.-L. Polym J 2000, 32, 348.
31. Li, X.-G.; Huang, M.-R.; Yang, Y.-L. Polymer 2001, 42, 3427.
32. Huang, M.-R.; Li, X.-G.; Yang, Y.-L. Polym Degrad Stab 2000, 71, 31.
33. Anand, J.; Palaniappan, S.; Sathyanarayana, D. N. Polymer 1998, 39, 6819.
34. Li, X.-G.; Waxy, L.-X.; Huang, M.-R. Synth Met 2001, 123, 435.
35. Varma, I.-K.; Veena, C. J Polym Sci Polym Chem Ed 1976, 14, 973.
36. Socrates, G. Infrared Characteristics Group Frequencies; John Wiley: Chichester, UK, 1980.
37. Gupta, R. R. Physical Methods in Heterocyclic Chemistry; General Heterocyclic Chemistry Series: John Wiley: Chichester, UK, 1984.
38. Li, X. G.; Waxy, L. X.; Huang, M. R. Polymer 2001, 42, 6095.
39. Raj, V.; Madheswari, D.; Mubarak Ali, M. J Appl Polym Sci 2011, 119, 2824.